

# Alternative structures for two-dimensional MEMS optical switches [Invited]

Victor O. K. Li

*Department of Electrical and Electronic Engineering, The University of Hong Kong,  
Hong Kong SAR, China*

*vli@eee.hku.hk*

C. Y. Li and P. K. A. Wai

*Photonics Research Center and Department of Electronic and Information Engineering,  
The Hong Kong Polytechnic University, Hong Kong SAR, China*

*enli@polyu.edu.hk; enwai@polyu.edu.hk*

RECEIVED 16 AUGUST 2004; REVISED 10 SEPTEMBER 2004;  
ACCEPTED 10 SEPTEMBER 2004; PUBLISHED 29 SEPTEMBER 2004

Two-dimensional (2-D) microelectromechanical system (MEMS) optical switches have the merits of easy fabrication and high reliability. Since the optical signal loss is mainly proportional to the length of signaling paths in the switches, current 2-D MEMS optical switches that use a crossbar structure have a rather limited number of ports. For larger 2-D MEMS optical switches, we may use nonrectangular topology switching fabrics to shorten the internal signaling path or to recollimate the optical signal segment by segment inside the switches. We discuss these approaches from the aspect of implementation and routing control complexity. © 2004 Optical Society of America

*OCIS codes:* 060.1810, 230.3990.

## 1. Introduction

Optical cross connects (OXC)s are important elements in wavelength-division multiplexing (WDM) networks and applications such as multiple-protocol lambda switching [1, 2] and optical burst switching [3]. Many technologies have been proposed for building OXC)s. Microelectromechanical system (MEMS) optical switches have attracted much attention because of their potential in building large OXC)s [4–6]. MEMS optical switches use mirrors to modify the routing paths of optical signals inside the switches. There are two types of MEMS optical switch: those with mirrors that can rotate and stop at multiple positions and those with mirrors that can have only binary positions. The first type of MEMS optical switch has smaller optical signal loss but requires rather complicated servo control systems for the mirror movements. Since the control of mirror movement precision becomes difficult if  $N$  is large, reliability and stability are the main concerns with this type of MEMS optical switch [5].

The second type of MEMS optical switch uses straightforward digital control circuits to drive the movements of mirrors. The mirrors can be fabricated on a single silicon substrate. The optical signal propagation is parallel to the surface that integrates the mirrors. These switches are often called two-dimensional (2-D) MEMS optical switches. The switching time of 2-D MEMS optical switches (the required time for establishing a connection between input–output ports) can be within 1 ms because simple control algorithms are used. In general, 2-D MEMS optical switches are more reliable, stable, and easily fabricated [7]. However, currently available 2-D MEMS optical switches have a rather small number of ports, e.g.,  $N \leq 32$ , because optical signals are transferred in free space inside MEMS

optical switches. They get divergence and lose their power along the propagation paths. Since the paths are longer for a larger number of ports  $N$ , we have to use a larger mirror so that sufficient optical signal power can be transferred from the input to the output ports [8–10]. Currently, 2-D MEMS optical switches use a crossbar structure. Although the crossbar structure has the advantages of being strictly nonblocking and easy to fabricate for small switches, the required mirror size grows rapidly with the number of ports  $N$ . The fabrication becomes difficult when  $N$  is large. Although multistage MEMS optical switches with a crossbar structure have been proposed [11], the shortcomings are the high optical signal loss and the high interconnection cost between stages [5]. Hence, alternatives to the crossbar structure are desired for 2-D MEMS optical switches.

In some cases, special traffic patterns such as setting up connections in opposite directions in pairs can help double the capacity of 2-D MEMS optical switches by slight modifications to the crossbar structure [12, 13]. In general, there are two approaches for increasing the number of ports  $N$  in 2-D MEMS optical switches. The first approach is to shorten the input-to-output path length so that larger  $N$  can be available for the same mirror size. This approach uses nonrectangular switching fabrics, e.g.,  $L$  and triangular shapes [14, 15]. Complicated routings for the optical signals inside the switches are also required [16]. Another approach is to divide the input-to-output paths into multiple individually recollimated segments [17, 18]. Extra collimating optical devices are needed, e.g., collimating lenses [17], or concave mirrors [18]. In principle, the mirror size can be independent of the input-to-output path length [18], but the number of ports  $N$  would still be limited by other factors such as the required number of mirrors, complexity of the optical signal routings, and the number of reflections to the optical signals. Owing to the demands of large reliable OXCs, in this paper we investigate the pros and cons of building large 2-D MEMS optical switches with these approaches.

In Section 2, we use MEMS optical switches with crossbar structure as an example for discussing the performance parameters that we use to compare the alternative switch structures. We then describe the switch structures in Subsection 3: Polygon cross connects (Subsection 3.A), nonrectangular topology switching fabrics (Subsection 3.B), the matrix switches with integrated micro lenses (Subsection 3.C), and the  $2 \times 2$  switching module approach (Subsection 3.D). A comparison of the alternative switch structures is given in Section 4. Finally, we conclude in Section 5.

## 2. Performance Parameters for Two-Dimensional MEMS Optical Switches

For clarity, we use MEMS optical switches with crossbar structure as an example. Figure 1 shows a  $4 \times 4$  MEMS optical switch with crossbar structure. Input ports and output ports are labeled from  $I_1$  to  $I_4$  and  $O_a$  to  $O_d$ , respectively. We label the mirrors according to their row–column position. Each mirror can either be in the ON or the OFF state. A mirror  $(x, y)$  in the ON state reflects the optical signal from input port  $I_x$  to output port  $O_y$ . The mirrors in the OFF state have no effect on the switching of optical signals. In MEMS optical switches with crossbar structure, at most one mirror should be in the ON state at each row or column. The mirrors  $(1, d)$ ,  $(2, b)$ ,  $(3, c)$ , and  $(4, a)$  in Fig. 1 are in the ON state. Optical signals from input ports  $I_1$ ,  $I_2$ ,  $I_3$ , and  $I_4$  are switched to output ports  $O_d$ ,  $O_b$ ,  $O_c$ , and  $O_a$ , respectively. In the following, we discuss the performance parameters that vary with the switch structures. Those fabrication-related parameters such as device switching time and driving voltage will not be included [19].

### 2.A. Number of Switching Elements

For cost and reliability, it is desirable to minimize the number of switching elements,  $K_{sw}$ . In an  $N \times N$  optical switch with crossbar structure, the number of required switching ele-

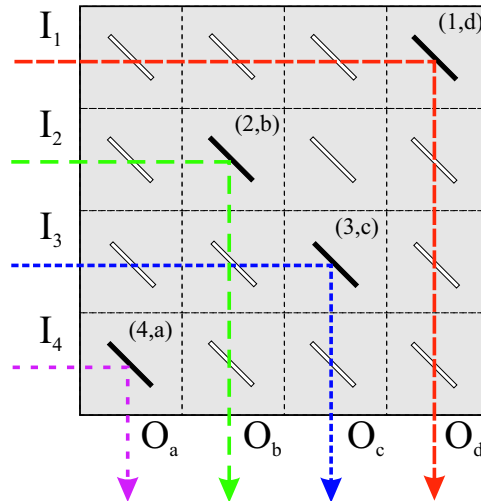


Fig. 1.  $4 \times 4$  2-D MEMS optical switch with crossbar structure. The mirrors (1,d), (2,b), (3,c), and (4,a) are in the ON state. Optical signals from input ports  $I_1$ ,  $I_2$ ,  $I_3$ , and  $I_4$  are switched to output ports  $O_d$ ,  $O_b$ ,  $O_c$ , and  $O_a$ , respectively.

ments (movable mirrors) is  $N^2$ . Most noncrossbar structures require fewer switching elements [20]. For example, the number of required  $2 \times 2$  switching modules in Spanke–Beneš [21] and Beneš [22] networks are  $N(N-1)/2$  and  $N \log_2 N - N/2$ , respectively. Since the function of a  $2 \times 2$  switching module is to pass or interchange the two input optical signals in a MEMS optical switch, one movable mirror is sufficient in each module. The savings of switching elements can be significant but often at the expense of higher routing complexity and more reflections to the optical signals.

## 2.B. Complexity of Optical Signal Routing

The complexity of routing the optical signals inside the switches can affect system performance if the complexity grows rapidly with the switch size. The MEMS optical switch with crossbar structure in Fig. 1 has a unique optical signal routing path for a given pair of input and output ports. All paths are formed by two segments. Since the optical signals are transferred in free space, different path segments can cross one another without interference. Only one mirror must be activated to set up a connection. These properties simplify optical signal routing inside the switches. The required processing for routing an optical signal inside the switching is a constant.

## 2.C. Optical Path Length

The path length  $P$  of optical signals is important, since the strength of the optical signals degrades with the path length. In Fig. 1, the path length  $P(x,y)$  of a connection  $I_x \rightarrow O_y$  is  $4 - x + y$  intermirror distance units (itches) if we relabel  $a, \dots, c$  to  $1, \dots, 4$ . In an  $N \times N$  MEMS optical switch with crossbar structure, internal path length can vary from 1 to  $2N - 1$ , e.g., the path lengths of connections  $I_4 \rightarrow O_a$  ( $P_{\min}$ ) and  $I_1 \rightarrow O_d$  ( $P_{\max}$ ) are 1 and 7, respectively. Since the outputs of a switch should have similar signal quality, the path-length difference between the connections should be as small as possible. Otherwise, extra effort is required for equalizing the optical signals.

## 2.D. Number of Reflections

In MEMS optical switches, the loss of optical signals increases with the number of reflections  $K_{\text{ref}}$  encountered inside the switches because of mirror angular misalignment and mirror imperfect reflection [8]. Since optical signals encounter only one reflection in crossbars, i.e.,  $K_{\text{ref}} = 1$ , we generally neglect the reflection-related optical signal losses in designing MEMS optical switches with crossbar structure. When structures other than crossbars are used, an optical signal may encounter multiple reflections before going to the desired output port. The optical losses resulting from reflection may be significant. The number of reflections,  $K_{\text{ref}}$ , in such situations becomes a helpful parameter for describing the difference between switch structures.

## 2.E. Loss of Optical Signals

When an optical signal passes through a MEMS optical switch, it encounters optical power loss in response to coupling loss between the fibers and the switch, mirror angular misalignment, imperfect mirror reflection, air absorption, and beam divergence [5, 8]. Coupling loss is invariant for all kinds and sizes of MEMS optical switch. Losses caused by mirror angular misalignments and mirror imperfections are often neglected because of the improvement in the MEMS fabrication process, e.g., angular misalignment  $< 0.1$  deg and commercial-grade mirror reflectivity  $> 98\%$  [19]. We consider them only if the number of reflections is large. Air absorption loss grows with the optical signal path length  $P$ , but it is insignificant when beam divergence loss is considered.

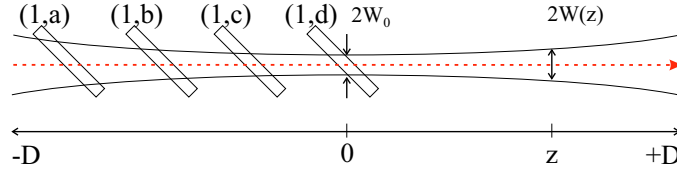


Fig. 2. Gaussian-beam model for the optical signal from input  $I_1$  of the switch in Fig. 1. Mirrors (1,a) to (1,d) are in the OFF state. The optical signal is collimated and focused onto the mirror (1,d).  $W(z)$  is the Gaussian-beam radius of the optical signal at distance  $z$ .

Figure 2 uses the connection  $I_1 \rightarrow O_d$  of Fig. 1 as an example to describe beam divergence. For illustration, we assume that mirror (1,d) is also in the OFF state. The distance between the input port  $I_1$  to mirror (1,d) is  $D$ . The coordinate 0 of the propagation distance is set at the location of mirror (1,d).  $W(z)$  is called the *Gaussian-beam radius* and represents the radius at which the optical signal intensity has dropped to  $\exp(-2) \approx 0.135$  of its maximum at distance  $z$  [23]. The optical loss resulting from Gaussian-beam divergence for a mirror of radius  $R$  at distance  $z$  is

$$L_{\text{Gauss}} = \exp \left[ -\frac{2R^2}{W(z)^2} \right]. \quad (1)$$

$W(z)$  can be calculated from

$$W(z) = W_0 \left[ 1 + \left( \frac{z}{z_0} \right)^2 \right]^{\frac{1}{2}}, \quad (2)$$

where  $W_0 = W(0)$  is the *waist radius*, which is the minimum value of  $W(z)$ . We assume that the optical signal is collimated and focused onto the midpoint of the optical path to

minimize the diffraction [5]. Otherwise,  $W_0$  will be at the location  $-D$  instead of the location 0. Here  $z_0$  is called the *Rayleigh range*, which is the distance  $z$  for  $W(z) = 2^{1/2}W_0$ .  $W_0$  and  $z_0$  are related as  $W_0 = (\lambda z_0/\pi)^{1/2}$ , where  $\lambda$  is the wavelength of the optical signal. In principle we may reduce  $L_{\text{Gauss}}$  by using large mirrors or small-beam-radius optical signals; e.g.,  $L_{\text{Gauss}}$  will be smaller than 1.1% if we use a mirror with radius  $R = 1.5W(z)$ . Owing to the fabrication limits, however, both the mirrors and the optical signal beams should be of reasonable size. The minimum value of  $W(D)$  is  $(2\lambda D/\pi)^{1/2}$  when we set  $z_0 = D$  in Eq. (2). In MEMS optical switches with crossbar structure,  $L_{\text{Gauss}}$  becomes significant if the number of ports  $N$  is large.

## 2.F. Mirror Radius

Mirror radius is highly related to optical signal loss and to the switch dimension. For power consumption and reliability, the mirrors should be small. However, it should be large for minimizing  $L_{\text{Gauss}}$ . Since the limitations of the fabrication process should also be considered, the situation becomes complicated. Equation (2) shows that the optical signal beam radius  $W(D)$  is proportional to the path length  $P$  ( $2D$  in Fig. 2). Since  $P_{\text{max}} = 2N - 1$  in MEMS optical switches with crossbar structure, large mirrors are therefore required for switches with large  $N$ . For  $N = 16$  and  $32$ , the mirror radii of MEMS optical switches with crossbar structure are approximately  $146$  and  $228 \mu\text{m}$ , respectively, if  $3R + 800 \mu\text{m}$  is used to approximate a pitch, i.e., the distance between mirrors, considering the fabrication process limitations [8]. The mirror size varying with the number of ports  $N$  also causes extra difficulties in fabrication of large MEMS optical switches.

Let  $\sigma$  be the ratio constant between the intermirror distance and the optical signal beam radius  $W(D)$ . The dimension of a MEMS optical switch with crossbar structure is then approximated as  $D \approx N\sigma W(D)$ . Since the minimum  $W(D)$  is  $(2\lambda D/\pi)^{1/2}$ , we have

$$D \approx 2N^2\sigma^2\lambda/\pi.$$

This implies that we should increase the switch dimension fourfold if we double the number of ports  $N$ . Otherwise, the optical signal loss resulting from Gaussian-beam divergence increases significantly. The switch dimension increasing rapidly with  $N$  makes MEMS optical switches with crossbar structure unattractive if  $N$  is large [9, 10].

## 2.G. Nonblocking Property

Two-dimensional MEMS optical switches with crossbar structure have a unique path between an input–output pair. The path setup does not interfere with the acceptance of new connections in other input–output pairs. This phenomenon is strictly nonblocking [22]. However, two or more paths may be available between an input–output pair if other switch structures are used. In such cases, the path setup may have to follow some rules to avoid interference in the later connection acceptance, i.e., wide-sense nonblocking. Some switch structures can be “rearrangeably” nonblocking; i.e., we may be required to rearrange the paths of existing connections in order to accept new connections. Rearrangeably nonblocking switches are not preferred in traditional telecommunication applications, because adding a new connection may disturb the existing connections. Besides, it may not be easy to rearrange the paths of existing connections within the connection setup time (typically seconds) if the switch size is large, e.g.,  $N > 10^4$  for general telephone systems. In WDM optical networks, the setup of connections is based on the demands of multiple gigabits-per-second bandwidth. The duration of a wavelength connection is relatively long compared with that for telephone connections. Since we can tolerate a longer connection setup time, it is possible to minimize the disturbance to existing connections even if rearrangeably nonblocking switches are used.

### 3. Alternative Switch Structures

Although MEMS optical switches with crossbar structure have the advantages of low control complexity, topology regularity, and easy fabrication, they require mirrors in large number, mirrors with large radius, and switching fabrics in large dimension. Otherwise, the optical signal loss grows rapidly with the number of ports. Alternative switch structures have been proposed to reduce the number of mirrors and lower the optical signal loss.

#### 3.A. Polygon Cross Connects

Without significantly increasing the hardware complexity, a simple way to double the capacity of a MEMS optical switch with crossbar structure is to take advantage of the connection symmetry property; i.e., connections are often set up in pairs [12, 13]. We can always relabel the input–output ports and use a switch to exchange the connections such that  $I_x \rightarrow O_y$  and  $I_y \rightarrow O_x$  are set up in pairs. The number of mirrors  $K_{sw}$  can therefore be largely reduced if we can switch the two connections with one mirror. From this idea, MEMS optical switches with modified crossbar structure using double-sided mirrors have been proposed and generalized to the Polygon cross connects to serve nodes with degree 3 or more [13]. Figure 3 shows a Polygon cross connect for a node with degree 3. Three trunk groups have been connected to the node. Input–output sets  $\{I_1/O_1, I_2/O_2\}$ ,  $\{I_3/O_3, I_4/O_4\}$ , and  $\{I_5/O_5, I_6/O_6\}$  belong to different trunk groups. Connections can be set up only between inputs and outputs in different trunk groups. All mirrors in Fig. 3 are double-sided. The mirrors (1,6), (2,3), and (4,5) are in the ON state. Optical signals from input ports  $I_1$ ,  $I_2$ ,  $I_3$ ,  $I_4$ ,  $I_5$ , and  $I_6$  are switched to output ports  $O_6$ ,  $O_3$ ,  $O_2$ ,  $O_5$ ,  $O_4$ , and  $O_1$ , respectively.

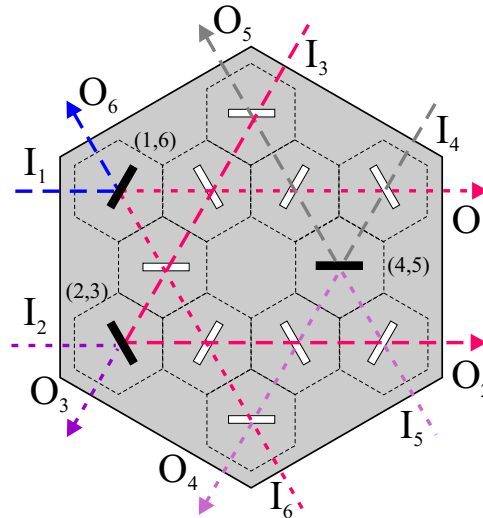


Fig. 3. Degree 3 Polygon 2-D MEMS optical cross connect that takes advantage of the connection symmetry property, i.e.,  $I_x \rightarrow O_y$  if  $I_y \rightarrow O_x$ . All mirrors are double-sided. The mirrors (1,6), (2,3), and (4,5) are in the ON state. Optical signals from input ports  $I_1$ ,  $I_2$ ,  $I_3$ ,  $I_4$ ,  $I_5$ , and  $I_6$  are switched to output ports  $O_6$ ,  $O_3$ ,  $O_2$ ,  $O_5$ ,  $O_4$ , and  $O_1$ , respectively.

With the connection symmetry property, the cross connect in Fig. 3 requires only 12 double-sided mirrors instead of the 24 mirrors used in MEMS optical switches with crossbar structure. To serve a  $d$ -degree node with  $n$  input–output pairs on each trunk group, a single MEMS optical switch with crossbar structure requires  $(nd)^2$  mirrors. If the signal transportations from a trunk group to other  $(d - 1)$  trunk groups are handled by a dedicated

$n \times (d-1)n$  switch, we need a total of  $d(d-1)n^2$  mirrors and  $d$  number of  $(d-1)$  to 1 couplers. Using the Polygon cross connect, we require only  $d(d-1)n^2/2$  mirrors.

### 3.B. Nonrectangular Topology Switching Fabrics

Although Polygon cross connects use double-sided mirrors to switch a pair of optical signals simultaneously, parameters such as optical signal loss, mirror size, and switch physical dimension are similar to those of the crossbars. Evidently, Polygon cross connects would encounter the problems similar to those of MEMS optical switches with crossbar structure if the number of connection pairs is large. Hence, nonrectangular topologies have been suggested for 2-D MEMS optical switches, e.g., the  $L$ -switching matrix [14] and the array interconnection [15, 16], to shorten the input-to-output path lengths instead of taking advantage of the connection symmetry property. An  $N \times N$  2-D MEMS optical switch with nonrectangular topology reduces the maximum input-to-output path length from  $\mathcal{O}(2N)$  to  $\mathcal{O}(1.5N)$  [14, 15]. The required mirror radius is therefore 0.866 that of the crossbars. We may use it to halve the  $L_{\text{Gauss}}$  and increase the number of ports  $N$ . In addition, nonrectangular topology 2-D MEMS optical switches can require half the number of mirrors as those with crossbar structure. These are done at the expense of multiple reflections to the optical signals, more-complicated routing control, and rearrangeably nonblocking property.

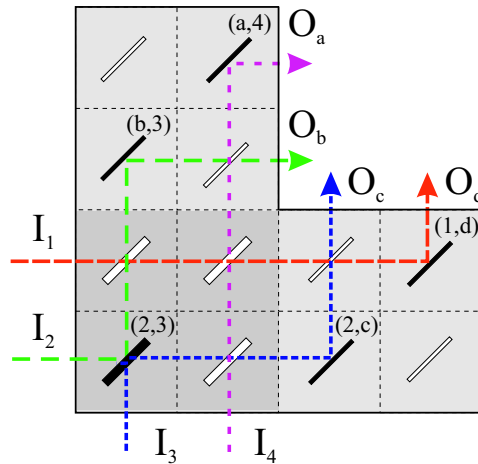


Fig. 4.  $4 \times 4$   $L$ -switching matrix 2-D MEMS optical switch. The input-output connections are the same as in Fig. 1. The mirrors in the dark-gray area are double-sided, while the rest can be single-sided mirrors. The mirrors (1,d), (2,3), (2,c), (a,4), and (b,3) are in the ON state. Multiple reflections are required for shortening the internal optical signal paths, e.g., two reflections for connections  $I_2 \rightarrow O_b$  and  $I_3 \rightarrow O_c$ .

Figure 4 shows a  $4 \times 4$   $L$ -switching matrix 2-D MEMS optical switch [14]. The input-output connections are the same as those in Fig. 1. Since the input-output ports and the mirrors are arranged according to the  $L$ -shape area, the maximum input-to-output distance is 5 instead of the 7 in Fig. 1. However, multiple reflections are required for switching the optical signals, e.g., two reflections for connections  $I_2 \rightarrow O_b$  and  $I_3 \rightarrow O_c$ . Since the connection symmetry is not assumed and some connections have to share mirrors, cooperation between mirrors is important. In Fig. 4, the mirrors in the dark-gray area are double-sided, whereas the rest can be single-sided mirrors. Without other connections, connection  $I_3 \rightarrow O_c$  has three choices of routing path and mirror setting. When the rest of the connections are considered, however, the feasible setting is only mirrors (1,d), (2,3), (2,c), (a,4), and (b,3) in the ON state. Otherwise, avoidable blocking occurs.



Apart from having shorter internal optical signal path lengths, 2-D MEMS optical switches with nonrectangular topologies require a smaller number of mirrors. An  $L$ -switching matrix requires  $N^2/4$  double-sided and  $N^2/2$  single-sided mirrors. The number of mirrors can be further reduced by arranging the input–output ports and mirrors according to a triangular area as that shown in Fig. 5 [15]. The maximum optical signal path length is still  $\mathcal{O}(1.5N)$ , but we require only  $N(N-1)/2$  movable double-sided and  $N$  fixed mirrors. The reduction of hardware complexity is at the cost of more reflections to the optical signals, e.g., three reflections instead of one are required for connections  $I_1 \rightarrow O_d$  and  $I_4 \rightarrow O_a$ .

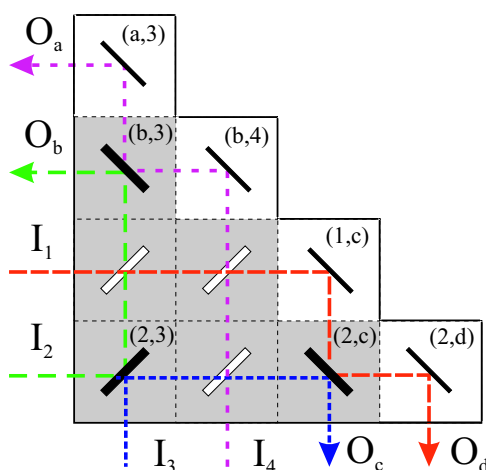


Fig. 5.  $4 \times 4$  rearrangeable nonblocking 2-D MEMS optical switch. The input–output connections are the same as in Fig. 1. Mirrors (2,3), (2,c), and (b,3) are in the ON state. All mirrors are double-sided apart from those in the white area, i.e., (a,3), (b,4), (1,c), and (2,d), which are nonmovable mirrors. More reflections are required for reducing the number of movable mirrors. For connections  $I_1 \rightarrow O_d$  and  $I_4 \rightarrow O_a$ , three reflections instead of one in Fig. 4 are required.

Two-dimensional MEMS optical switches with nonrectangular topology are rearrangeably nonblocking. Algorithms have been proposed to ensure that new connections can always be accepted when there are no existing connections [16]. In some cases, we have to reroute existing connections to accept a new connection. Otherwise, the new connection may encounter a large number of reflections or, in the worst case, be blocked. Without existing connections, a new connection encounters at most three reflections on its path from input to output in a nonrectangular topology 2-D MEMS optical switch, e.g., see Fig. 5. However, up to hundreds of reflections may be required if existing connections are considered [16]. It is a challenge to develop fast algorithms that balance the disturbance to existing connections and the number of reflections to optical signals.

### 3.C. Matrix Switches with Integrated Microlenses

Owing to the high complexity of routing control and the rearrangeably nonblocking property, nonrectangular topology 2-D MEMS optical switches may not be suitable for some applications. Instead of modifying the switching fabric topology, an alternative is to control the optical signal beam radius with microcollimating lenses and increase the maximum size of MEMS optical switches with crossbar structure accordingly [17]. There are two approaches. The first is to integrate a collimating lens on each mirror of a MEMS optical switch with crossbar structure. In MEMS optical switches with crossbar structure, optical



signals are collimated and focused to the farthest mirrors to minimize the required mirror radius, e.g., the minimum optical signal beam radius  $W_0$  is at location 0 in Fig. 2. By integration of the lenses on the mirrors, however, the minimum optical beam size should be set at the midpoint of the path to the farthest mirrors instead, e.g., the location  $-D/2$  in Fig. 2. In principle, this can double the maximum path length of the optical signals or reduce the mirror radius to 0.707 of the original if each lens can be tailor-made for the corresponding set of mirror and input–output ports. Since the lens radius can be a few tens of the optical wavelength, traditional design rules may no longer be applicable for the lenses. Moreover, the large incidence angle (45 deg) also makes techniques such as paraxial and Gaussian-beam approximations inaccurate for modeling the action of the lens on the optical beam [24]. Direct simulation of the interaction of the optical beam and the mirror lens system by solving the Maxwell equations with techniques such as the finite-difference time-domain (FDTD) method is not feasible either because of the size of the mirror lens systems. The suitable parameters for the mirror lens system may have to be determined by experiments, and fabrication of the switches will be rather complicated.

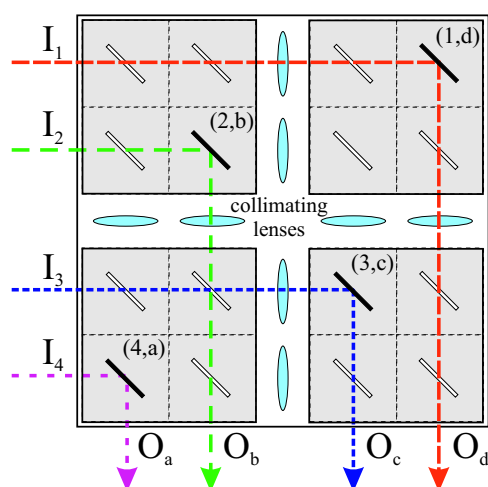


Fig. 6.  $4 \times 4$  multimodule 2-D MEMS optical switch with crossbar structure. The input–output connections and status of the mirrors are the same as in Fig. 1. There are four  $2 \times 2$  MEMS switching modules with crossbar structure. Intermodule collimating lenses are used to extend the path length limit of the optical signals. Another proposal is to integrate lens on each mirror instead of the intermodule lens arrays.

Another approach is to install collimating lens arrays between the MEMS switch modules as shown in Fig. 6 [17]. Figure 6 is a  $4 \times 4$  multimodule 2-D MEMS optical switch with crossbar structure. There are four  $2 \times 2$  MEMS switching modules with crossbar structure similar to that in Fig. 1. The collimating lenses are used only to reduce the beam radius of the optical signals between modules. The required number of collimating lenses is therefore largely reduced. Separating lenses and mirrors also simplifies the fabrication process. Lens design, however, is more complicated because the optical signals may pass through multiple switching modules and lenses. The lenses have to be carefully designed to optimize for the various conditions. Otherwise, the performance of the optical switches will degrade significantly.

### 3.D. $2 \times 2$ Switching Module Approach

All MEMS optical switches we discussed in Subsections 3.A, 3.B, 3.C still have the problem that their number of input–output ports are limited by the acceptable maximum input–

to-output path length. Using a mix of the approaches may increase the number of input–output ports in some cases, but the problem persists. One way to solve the problem is to segment the paths inside the switches and collimate the optical signals segment by segment [18]. From Subsection 2.E, an optical signal with wavelength  $\lambda$  has a minimum beam radius  $(2\lambda D/\pi)^{1/2}$  at the midpoint of a free-space propagation path of length  $2D$  if it has been collimated and focused onto the path midpoint. The acceptable maximum path length of the optical signals is determined once the mirror size is given. The maximum number of input–output ports then depends on how we arrange the input–output ports and the mirrors [13–16]. Integrating lenses on mirrors of the MEMS optical switches with crossbar structure (Subsection 3.C) increases the acceptable maximum input-to-output optical path length by dividing the paths into two individually collimated segments. However, the acceptable maximum length of each segment is still limited by the mirror size [17]. Since the input-to-output path length grows with the number of input–output ports, we need solutions that adaptively divide the optical paths into segments with lengths that do not grow or only grow slowly with the number of input–output ports. Furthermore, routing of the optical signals inside the switches should be as simple as possible. One simple solution is to borrow from the traditional wisdom of building large switches by decomposing them into networks of  $2 \times 2$  switching modules [20]. For example, Fig. 7 shows two  $4 \times 4$  switches using architectures of Spanke–Beneš [21] and Beneš networks [22]. As the performance and operation of these networks have been well studied, the remaining problem is to implement the  $2 \times 2$  switching modules with MEMS.

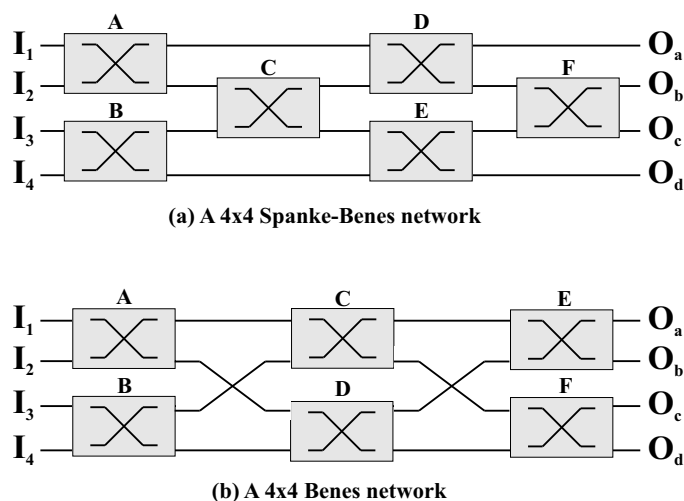


Fig. 7. Two rearrangeably nonblocking switch architectures. (a)  $4 \times 4$  Spanke–Beneš network. (b)  $4 \times 4$  Beneš network.

Figure 8 shows a proposed design of  $2 \times 2$  switching modules [18]. In the center of the  $2 \times 2$  switching module, there is a movable double-sided flat mirror  $M_{sw}$  for exchanging the optical signals. Unlike the approach we described in Subsection 3.C, there are no extra collimating lenses.  $M_1$ ,  $M_2$ ,  $M_a$ , and  $M_b$  are input and output fixed concave mirrors that not only direct but also collimate the optical signals between  $2 \times 2$  switching modules. For a pair of connected  $2 \times 2$  switching modules in neighboring stages, their output and input mirrors must be matched so that the optical signals can be appropriately recollimated. Assuming that the ON–OFF status of mirror  $M_{sw}$  has a negligible effect, the optical beam sizes are determined by their propagation distance between the  $2 \times 2$  switching modules and are not related to the optical path length from input-to-output ports. Hence, large 2-

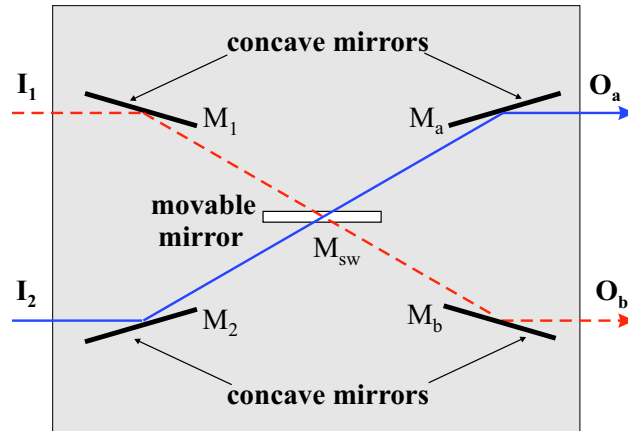


Fig. 8. Proposed  $2 \times 2$  switching module in cross state. The two optical signals from inputs  $I_1$  and  $I_2$  will be switched to the outputs  $O_b$  and  $O_a$ , respectively, if the movable switch is in the OFF state. Otherwise, optical signals from inputs  $I_1$  and  $I_2$  are switched to outputs  $O_a$  and  $O_b$ , respectively.

D MEMS optical switches can be built accordingly. In some network architectures, e.g., the Spanke–Beneš networks in Fig. 7(a) [21], the optical signal propagation distance is constant for most pairs of  $2 \times 2$  switching modules in neighboring stages. Similar to the case of the mirror lens system in Subsection 3.C, the suitable parameters for the concave mirrors  $M_1$  to  $M_b$  may have to be determined by experiments because of the difficulties in modeling the reflected optical beams under large incidence angles and small mirror radius [25]. Fabrication of mirrors to a predetermined radius of curvature and tolerance is certainly not easy. The fabrication process for the Spanke–Beneš architecture is simpler than that of the Beneš architecture because the intermodule distance is the same and most of the  $2 \times 2$  switching modules are identical for the former architecture, i.e., most of the concave mirrors have the same radius of curvature.

We can build large MEMS optical switches with a  $2 \times 2$  switching module, but the switch performance largely depends on the switch architectures. Although many  $2 \times 2$  switching-module-based switch architectures are available for different purposes, few of them are designed for MEMS optical switches. For example, Spanke–Beneš networks have the shortest optical signal propagation distance between neighboring  $2 \times 2$  switching modules but require  $N(N-1)/2$  switching modules for an  $N \times N$  switch [21]. In contrast, Beneš networks require only  $N \log_2 N - N/2$  switching modules, but the optical signal propagation distances between modules can be large, and change with the location of the modules and the switch size [22]. To strike a balance, we may either combine the input–output mirrors of the two  $2 \times 2$  switching modules in neighboring stages of the Spanke–Beneš networks to save mirrors or add more mirrors to further divide a long segment in Beneš networks so that small mirrors can be used. In most cases, we may have to modify the existing  $2 \times 2$  switching-module-based switch architectures to provide the required performance. New switch architectures may be required in some cases.

#### 4. Comparison between Different Switch Structures

The comparisons between different 2-D MEMS optical switch structures are summarized in Table 1. For a fair comparison, we use a Polygon cross connect (Subsection 3.A) with  $N$ -pair connections, i.e.,  $M = 2N$  input–output ports with connection symmetry. For non-rectangular topology switching fabrics, we assume a triangular shape [15]. For the matrix

switches in Subsection 3.C, we assume that a lens is integrated onto each mirror. Hence, the maximum performance from this kind of switch can be obtained [17]. For the  $2 \times 2$  switching module approach in Subsection 3.D, both the results of the Spanke–Beneš and Beneš architectures are listed.

In Table 1, we compare alternative architectures under those different parameters, not including the optical loss. As we discussed in Subsection 2.E, the optical losses caused by coupling, mirror imperfections, and misalignments depend highly on the fabrication processes. We assume that they are negligible owing to the improved MEMS technology [19]. For the beam divergence loss, a new performance model other than that in Subsection 2.E is required for correctly describing the reflected beams by the mirror lens system in Subsection 3.C and the concave mirrors in Subsection 3.D. Such a model, however, is not available at the moment. Since the beam divergence loss highly depends on the radii ratio between optical beams to that of the mirrors, mirror radius in Table 1 is also used to represent the optical loss performance of optical switches in ideal cases. For a detailed comparison, the required mirror radii for different switch structures ignoring the effect of large incidence angles are plotted in Fig. 9. The mirror radius is set to 1.5 of the maximum beam radius of the optical signals in the maximum input-to-output path of the switches. Switch structures that require smaller mirrors have a larger reduction in beam divergence loss (Section 2). For convenience, the pitch size between mirrors is set to the approximation  $3R + 800 \mu\text{m}$  for all switches, where  $R$  is the mirror radius [8]. Figure 9 shows the required mirror radii in micrometers for the MEMS optical switches we described in Sections 2 and 3 except for the Polygon cross connect. The Polygon cross connect can be treated as a MEMS optical switch with crossbar structure if we consider connections in only one direction. The mirror radii for the optical switches with structures of crossbars, nonrectangular switching fabrics, and crossbars with collimating lenses are plotted with the dotted, dashed, and dashed-dotted curves, respectively. Those for the  $2 \times 2$  switching modules with Beneš and Spanke–Beneš architectures are plotted with solid curves with crosses and circles, respectively. From Fig. 9, the switches using the  $2 \times 2$  switching module approach with Spanke–Beneš architecture require a mirror radius that is independent of the number of ports  $N$ , whereas those of the switches with crossbar structures increase rapidly. Those with other switch structures require a mirror radius that is in between these two. The mirror size of the Spanke–Beneš architecture does not vary with the number of ports because the intermediate distance is constant and the concave mirrors are used to collimate the optical beams. But this is achieved at the expense of the largest number of reflections to the optical signals  $3N$ , large number of mirrors  $N(N-1)/2$ , and large routing complexity  $\mathcal{O}(N^2/2)$ . If these problems could be overcome with improved MEMS fabrication processing, the  $2 \times 2$  switching module approach with Spanke–Beneš architecture would be the best choice.

**Table 1. Comparison between 2-D MEMS Optical Switch Structures**

	Crossbar	Polygon	Nonrectangular	Lensed Crossbar	2 × 2 SW Module	
					Spanke-Beneš	Beneš
Mirror radius <sup>(b)</sup>	$\infty 2N$	$\infty M^{(c)}$	$\infty 1.5N$	$\infty N$	Constant	$\infty N$
Max. number of reflections	1	1	$2N - 1^{(d)}$	1	$3N$	$6\log_2 N - 3$
Number of movable mirrors	$N^2$	$M^2/4^{(c)}$	$N(N - 1)/2$	$N^2$	$N(N - 1)/2$	$N\log_2 N - N/2$
Number of fixed mirrors <sup>(e)</sup>	0	0	$N$	0	$2N(N - 1)$	$4N\log_2 N - 2N$
Routing complexity <sup>(f)</sup>	$\mathcal{O}(N)$	$\mathcal{O}(M/2)^{(c)}$	$\mathcal{O}(N^2/2)$	$\mathcal{O}(N)$	$\mathcal{O}(N^2/2)$	$\mathcal{O}(N\log_2 N)$
Max. path length (pitches)	$2N - 1$	$M - 1^{(c)}$	$1.5N$	$2N - 1$	$N$	$N$
Blocking property <sup>(g)</sup>	SNB	SNB	RNB	SNB	RNB	
Mirror reflection sides	Single	Double	Double	Single	Double	
Mirror type <sup>(h)</sup>	Flat	Flat	Flat	Flat	Flat and concave	
Extra collimating lenses	No	No	No	Yes	No	
Connection symmetry	No	Yes	No	No	No	

<sup>(a)</sup> Crossbar: the 2-D MEMS optical switches with crossbar structure (Section 2). Polygon: the Polygon cross connects (Subsection 3.A). Nonrectangular: the Nonrectangular topology switching fabrics (Subsection 3.B). Lensed crossbar: Matrix switches with integrated microlenses (Subsection 3.C). 2 × 2 SW module: 2 × 2 switching modules (Subsection 3.D).

<sup>(b)</sup> Optical signals are collimated to the midpoint of the segments to minimize the required mirror size.

<sup>(c)</sup> For fair comparison,  $M = 2N$ .

<sup>(d)</sup> The LB (least-bend) routing algorithm is used [16].

<sup>(e)</sup> Both flat and concave mirrors are considered.

<sup>(f)</sup> The computations required for setup  $N$  connections.

<sup>(g)</sup> SNB is strictly nonblocking; RNB is rearrangeably nonblocking.

<sup>(h)</sup> Only flat or concave mirrors are considered here.

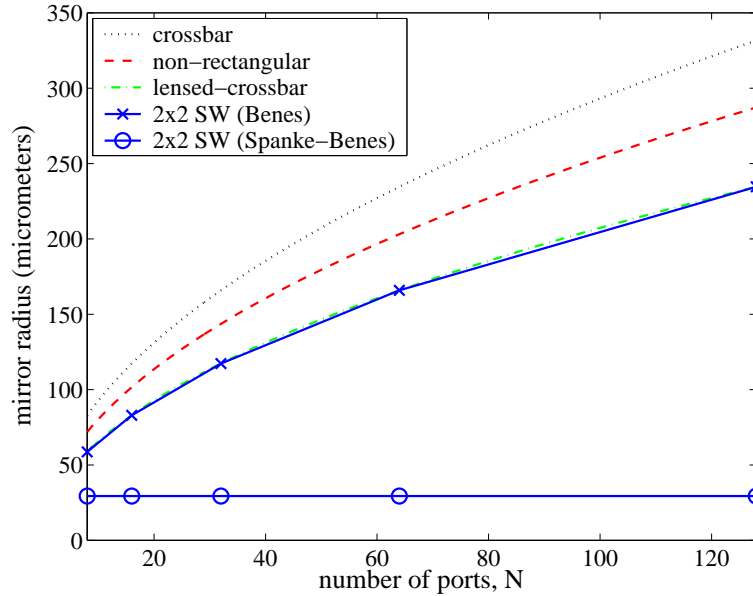


Fig. 9. Required radius of mirrors for 2-D MEMS optical switches with the structures of crossbars, nonrectangular topology fabrics, crossbar with collimating lenses, and  $2 \times 2$  modules with Beneš and Spanke-Beneš architectures.

The routing complexity is not important in crossbar-like switch structures (including Polygon cross connects and crossbar structures with collimating lenses), but it may cause significant performance degradation for noncrossbar structures (both nonrectangular topology fabrics and the  $2 \times 2$  switching module approach). Only the complexity of  $\mathcal{O}(N)$  is required for routings in crossbar-like switch structures. Moreover, these structures are strictly nonblocking and have at most one reflection to the optical signals. In non-crossbar-like structures, we are required to minimize the reflections as well as the disturbance to the existing connections. We may have to block the new connections if we cannot find the suitable paths within the setup period. Routing algorithms that demand heavy computations are not favorable even if they have better path searching capability. From Table 1, the maximum routing complexity of non-crossbar-like structures is  $\mathcal{O}(N^2/2)$ . Since this computational complexity considers the path searching only for new connections, the application of the noncrossbar structures may be restricted if the rerouting of existing connections is considered. Similar to our discussion in Subsection 3.B, fast algorithms that can balance the disturbance to existing connections and the number of reflections to optical signals are useful in the application of non-crossbar-like structures.

MEMS optical switches using the  $2 \times 2$  switching module approach with Beneš architecture require  $N \log_2 N - N$  movable double-sided flat mirrors and  $4N \log_2 N - 2N$  fixed concave mirrors. The required mirror size is similar to that of the crossbar with collimating lenses. Movable double-sided flat mirrors have been demonstrated in prototypes of Polygon cross connects [13] and the  $L$ -switching matrix [14]. The fabrication of concave mirrors is feasible but requires complicated etching and micromachining processing [19]. As we have discussed in Subsection 3.D, suitable parameters for the collimating devices may have to be determined by experiments at the moment [24, 25]. Since most switching modules in MEMS optical switches using the  $2 \times 2$  switching module approach with Spanke-Beneš architecture have similar parameters, we may have smaller fabrication complexity even though the required number of mirrors is larger.

## 5. Conclusion

MEMS technology is a mature technology for building large optical cross connects. Two-dimensional MEMS optical switches are reliable, stable, and easily fabricated but available only in a small number of input–output ports, e.g.,  $N < 32$ . The major limiting factor is that the size of mirrors inside the switches is proportional to the length of the paths that the optical signals take from the input to output ports. There are two approaches to increasing the number of ports for 2-D MEMS optical switches. The first approach is to shorten the input-to-output optical path length so that larger  $N$  can be available for the same mirror size. Another approach is to divide the input-to-output paths into multiple individually recollimated segments. Extra collimating optical devices are needed with this approach. In this paper, we have reviewed and compared different proposals including the Polygon cross connects, nonrectangular topology switching fabrics, crossbars with collimating lenses, and the  $2 \times 2$  switching module approach. If the problem of large number of reflections to optical signals could be overcome with improved MEMS fabrication processing, the  $2 \times 2$  switching module with Spanke–Beneš architecture would be the best choice. Otherwise, we may consider the Beneš architecture or the crossbar with collimating lenses.

## Acknowledgments

This research was supported in part by the Areas of Excellence Scheme established under the University Grants Committee of the Hong Kong Special Administrative Region, China (Project No. AoE/E-01/99). Additional support was provided by a grant from The Hong Kong Polytechnic University (Project Number A-PF98).

## References and Links

- [1] A. Banerjee, L. Drake, L. Lang, B. Turner, D. Awduche, L. Berger, K. Kompella, and Y. Rekhter, "Generalized multiprotocol label switching: an overview of signaling enhancements and recovery techniques," *IEEE Commun. Mag.* **39**, 144–151 (2001).
- [2] See <http://david.com.dtu.dk/>.
- [3] C. Qiao and M. Yoo, "Optical burst switching (OBS)—a new paradigm for an optical Internet," *J. High Speed Netw.* **8**, 69–84 (1999).
- [4] A. Neukermans and R. Ramaswami, "MEMS technology for optical networking applications," *IEEE Commun. Mag.* **39**, 62–69 (2001).
- [5] L. Y. Lin and E. L. Goldstein, "Opportunities and challenges for MEMS in lightwave communications," *J. Sel. Top. Quantum Electron.* **8**, 163–172 (2002).
- [6] X. H. Ma and G. S. Kuo, "Optical switching technology comparison: optical MEMS vs. other technologies," *IEEE Commun. Mag.* **41**, S16–S23 (2003).
- [7] P. De Dobbelaere, K. Falta, and S. Globeckner, "Advances in integrated 2D MEMS-based solutions for optical network applications," *IEEE Commun. Mag.* **41**, S16–S23, (2003).
- [8] L.Y. Lin, E.L. Goldstein, and R.W. Tkach, "On the expandability of free-space micromachined optical cross connects," *J. Lightwave Technol.* **18**, 482–489 (2000).
- [9] R. Ryf, D. T. Neilson, and C. R. Giles, "Scalable micro mechanical optical crossconnects," in *Micro- and Nano-optics for Optical Interconnection and Information Processing*, M. R. Taghizadeh and H. Thienpont, eds., *Proc. SPIE* 4455, 51–58 (2001).
- [10] B. Blau and K. Loesch, "The scalability of photonic switches," *Comput. Rendus Phys.* **4**, 75–83 (2003).
- [11] G. X. Shen T. H. Cheng, S. K. Bose, L. Chao, and Y. C. Teck "Architectural design for multistage 2-D MEMS optical switches," *J. Lightwave Technol.* **20**, 178–187 (2002).
- [12] J. M. Simmons, A. A. M. Saleh, E. L. Goldstein, and L. Y. Lin, "Optical crossconnects of reduced complexity for WDM networks with bidirectional symmetry," *IEEE Photon. Technol. Lett.* **10**, 819–921 (1998).



- [13] L. Y. Lin, E. L. Goldstein, J. M. Simmons, and R. W. Tkach, "High-density micromachined Polygon optical crossconnects exploiting network connect-symmetry," *IEEE Photon. Technol. Lett.* **10**, 1425–1427 (1998).
- [14] T. W. Yeow, K. L. E. Law, and A. A. Goldenberg, "SOI-based 2-D MEMS *L*-switching matrix for optical networking," *J. Sel. Top. Quantum Electron.* **9**, 603–613 (2003).
- [15] G. X. Shen, T. H. Cheng, C. Lu, T. Y. Chai, and S. K. Bose, "A novel rearrangeable non-blocking architecture for 2D MEMS optical space switches," *Opt. Netw. Mag.* **3**, 70–78 (2002).
- [16] T. Y. Chai, T. H. Cheng, S. K. Bose, C. Lu, and G. X. Shen, "Array interconnection for rearrangeable 2-D MEMS optical switch," *J. Lightwave Technol.* **21**, 1134–1140 (2003).
- [17] S. Gloeckner, A. Husain, and L. Fan, "Optomechanical matrix switches including collimator arrays," WIPO patent 0073842 (7 December 2000).
- [18] C. Y. Li, G. M. Li, V. O. K. Li, P. K. A. Wai, H. Xie, and X. C. Yuan, "Using  $2 \times 2$  switching modules to build large 2-D MEMS optical switches," in *Proceedings of IEEE Global Telecommunications Conference* (IEEE, New York, 2003), pp. 2789–2802.
- [19] D. Dragoman and M. Dragoman, "Micro/nano-optoelectromechanical systems," *Prog. Quantum Electron.* **29**, 229–250 (2001).
- [20] R. A. Spanke, "Architectures for guided-wave optical space switching systems," *IEEE Commun. Mag.* **25**, 42–48 (1987).
- [21] R. A. Spanke and V. E. Beneš, "*N*-stage planar optical permutation network," *Appl. Opt.* **26**, 1226–1229 (1987).
- [22] V. E. Beneš, *Mathematical Theory of Connecting Networks and Telephone Traffic* (Academic, New York, 1965).
- [23] B. E. A. Saleh and M. C. Teich, *Fundamentals of Photonics* (Wiley New York, 1991).
- [24] N. Lindlein, "Simulation of micro-optical systems including microlens arrays," *J. Opt. A: Pure Appl. Opt.* **4**, S1–S9 (2002).
- [25] S. P. Han, J. T. Kim, S. W. Jung, S. H. Ahn, C. G. Choi, and M. Y. Jeong, "A reflective curved mirror with low coupling loss for optical interconnection," *IEEE Photon. Technol. Lett.* **16**, 185–187 (2004).